NO_x enhancements in the middle atmosphere during 2003-2004 polar winter: The relative significance of Solar Proton Events and the Aurora as a source.

Annika Seppälä
Earth Observation, Finnish Meteorological Institute, Helsinki, Finland
Mark A. Clilverd
Physical Sciences Division, British Antarctic Survey, Cambridge, United Kingdom
Craig J. Rodger
Department of Physics, University of Otago, Dunedin, New Zealand

Abstract. In this study we combine odd nitrogen (NO_x) observations from the GOMOS and POAM III instruments with a radio wave ionisation index to provide a detailed description of the generation and descent of polar NO_x into the upper stratosphere during the northern hemisphere winter of 2003-2004. The measurements are used to study the relative contributions of ionization due to solar proton events, energetic electron precipitation, and low energy (1-10 keV) electron precipitation on NO_x production, and its subsequent downward transport to the upper stratosphere. We show that NO_x generated from the large solar proton storm in October/November 2003 was transported into the upper stratosphere in agreement with model calculations, but that aurorally generated NO_x also descended later in the winter. Both periods were highly significant and produced large long-lived decreases in stratospheric ozone once it arrived at those altitudes. The observations made by GOMOS deep into the nighttime polar vortex are critical in differentiating between the stratospheric effects of these two events.

1. Introduction

Precipitating charged particles produce odd nitrogen NO_x (NO + NO_2) in the Earth's atmosphere. The production altitude depends on the energy of the particle involved. The NO_x is typically generated in the region of the geomagnetic poles because the majority of particle precipitation occurs at these latitudes as a result of the influence of the Earth's magnetic field configuration. The high latitude polar vortex formed at the winter pole isolates the polar air in the upper stratosphere and mesosphere allowing any NO_x produced at high altitudes to be transported downward with the descending vortex air [Solomon et al., 1982; Manney et al., 2005]. Recently several studies have presented observed NO_x enhancements in the middle atmosphere as a result of downward transport from the upper atmosphere, and in some cases, following large solar storms [Seppälä et al., 2004; Randall et al., 2005; Lopez-Puertas et al., 2005; Funke et al., 2005].

During the northern hemisphere winter of 2003-2004 there were several significant solar proton events (including the Halloween storm in October/November 2003), geomagnetic storms, and a strong upper stratospheric polar vortex. High concentrations of NO_x were observed descending into the stratosphere in April 2004 from above [e.g., Randall et al, 2005], although it was unclear if the original source of the NO_x was from the solar protons, or relativistic electrons from a specific geomagnetic storm, or from the accumulation of NO_x production from all of the storms. The relatively low energy electrons that also produce the aurora (Energies 1-10 keV) generate NO_x at ~120 km altitude, solar proton events lead to strong NO_x enhancements below 80 km altitude [Jackman et al. 2005, Lopez-Puertas et al. 2005, Verronen et al., 2005], while relativistic electrons will produce NO_x enhancements at roughly 60-80 km. Any of these NO_x enhancements could then be transported downward into the upper stratosphere, as observed in April 2004. Note that all electrons forming NO_x above 100 km will be referred to in the present paper as "low energy electrons" and NO_x generated by low energy electron precipitation as LEE-NO_x. Note also that energy spectra caused by solar wind and CME effects may be such that significant NO_x

can be formed from the thermosphere down to about 75 km (In the thermosphere NO_y is also formed by soft x-rays and extreme ultraviolet radiation).

Semeniuk et al. [2005] used a middle atmosphere GCM to investigate the contribution of the Halloween storm (proton and electron precipitation) to stratospheric NO_x concentrations. Significant levels of NO_x were produced by the storm and descended to the upper stratosphere by early-December 2003, with concentration levels at 40 km being about 3× the background values. Although this timing was well before the satellite-observed April arrival of NO_x at stratospheric altitudes it was postulated that the modelled descent rates could have been reduced in reality by the stratospheric warming event that took place towards the end of December 2003. Renard et al. [2006] proposed that relativistic electron precipitation during the geomagnetic storm of 22 January 2004 was responsible for in-situ production of NO_x at ~60 km, which then descended to the upper stratosphere (~40 km) by April 2004 with NO_x concentrations that were 4× higher than background [Randall et al., 2005]. However, Clilverd et al. [2006] showed that the production of the NO_x in this time period originated at altitudes >90 km and thus the NO_x generation mechanism was more consistent with lower energy auroral electron precipitation at ~120 km. In addition, this study showed that the NO_x generation must have occurred before the 22 January 2004 geomagnetic storm, and after the Halloween storm. Recently Hauchecorne et al. [2007] have shown observations of an intense mesospheric warming in the northern polar region in mid-January 2004. In agreement with Clilverd et al. [2006], the results of Hauchecorne et al. [2007] indicate a strong air descent in the polar vortex resulting in descent of large quantity of NO from the upper mesosphere – lower thermosphere into the lower mesosphere.

The relative significance of Solar Proton Events and the aurora as a source of the high amounts of NO_x descending into the upper stratosphere is clearly an unanswered question. Was the Halloween storm proton event the most significant event in creating the descending NO_x, or was the production of NO_x from low energy electrons over an extended period of time more significant? In this paper we report GOMOS, POAM III, and radio wave observations of the polar middle atmosphere ozone and NO_x from October 2003 until the end of April 2004. We will focus on the observation and descent of a NO_x enhancement, caused by energetic particle precipitation during the Halloween storm, compared with the relative stratospheric impact of NO_x generated by low energy electrons, that descended later in the winter period.

2. Experimental setup

GOMOS measurements

One of the new instruments observing the polar night atmosphere is GOMOS (Global Ozone Monitoring by Occultation of Stars). Flying on board the Envisat satellite, GOMOS measures vertical profiles of several minor gases making up to 600 occultations per day with good global coverage [Kyrölä et al., 2004]. Since the launch of Envisat on 2002, the instrument has performed approximately 350 000 successful occultation measurements from 2002 up to early 2006.

In this study we have used GOMOS measurements (GOPR version 6.0c) from the Northern Hemisphere (NH) from October 2003 to March 2004. The altitude range and error of GOMOS measurements depend on the star temperature and magnitude. Based on discussions with the GOMOS team, we have selected stars with temperatures ≥6000 K for both NO_2 and O_3 measurements. In addition, we require the solar zenith angle at the tangent point to be >107°, and >90° at the satellite point, to avoid stray light conditions. GOMOS observations of NO_x have been discussed by [Hauchecorne et al., 2005], while O_3 has been discussed by [Kyrölä et al., 2006]. In the stratosphere the NO_x gases are in photochemical balance during the daytime. After sunset NO is quickly converted into NO_2 in reaction with O_3, and thus the nighttime NO_2 measurements used in this study are a reasonable representation of stratospheric NO_x. The quality of selected GOMOS measurements are discussed in more detail in the Appendix.

POAM III measurements

The POAM (Polar Ozone and Aerosol Measurement) III instrument was launched onboard the SPOT-4 spacecraft in March 1998. The instrument measures solar extinction in nine narrow band channels, covering the spectral range from approximately 350 to 1030 nm employing the solar occultation technique. POAM III provides vertical profiles of ozone (15-60 km), nitrogen dioxide (20-45 km), aerosol extinction, and water vapor in the polar stratosphere and troposphere with a vertical resolution of 1-2 km [Randall et al., 2002, 2003]. The POAM III retrieval version 4 includes ancillary profiles of temperature, pressure, and potential vorticity from the Met Office, interpolated to the location and time of the POAM III measurements. The MSISE-90 model [Hedin, 1991] has been used to extend these profiles above the top Met Office pressure level.

POAM III uses solar occultation, and therefore cannot make nighttime measurements, restricting the POAM observations to measurements outside of the polar night. In addition, the SPOT-4 spacecraft is in a sun-synchronous orbit, such that the solar occultation measurement is made at a single location (latitude and local time) each orbit, the latitude of which varies slowly with time. This is in contrast with the GOMOS stellar occultation technique, which provides multiple nighttime latitude/longitude measurements in each orbit.

Radio wave measurements

Very Low Frequency (VLF) radio signals, generated by transmitters located around the world, propagate in a waveguide formed by the Earths surface and the bottom of the ionosphere located between 50 and 100 km. Therefore all changes in this part of the ionosphere lead to changes in the amplitude and phase of received VLF signals. As a consequence of the sensitivity to changes in the lower ionosphere, VLF signals may be used to monitor changes in the sources of ionization, such as particle precipitation, in the mesosphere-lower thermosphere [see e.g. Clilverd et al. 2005 and references therein].

Here we use narrow-band subionospheric LF data from a 37.5 kHz transmitter (call sign NRK, 64ºN, 22ºW, *L*=5.6) located in Iceland and received at Ny Ålesund, Svalbard (79ºN, 11ºE, *L*=18.3). This site is part of the Antarctic-Arctic Radiation-belt Dynamic Deposition VLF Atmospheric Research Konsortia (AARDDVARK). The whole transmitter to receiver propagation path is well inside the region enclosed by a typical strong northern hemisphere upper stratospheric midwinter vortex, and would thus experience high latitude particle precipitation effects as well as changes in NO_x.

Previous work [Clilverd et al., 2006; Clilverd et al., 2007] has shown that the ionisation of NO in the mesosphere by Lyman-alpha radiation influences the propagation of radio wave signals received from the Iceland transmitter. A simple index provided by the difference between the average daytime amplitude of the received signal and the average nighttime amplitude is enough to identify the presence of ionisation caused by either precipitating protons/electrons or enhanced levels of NO.

3. Results

The two day running averages of the NO_2 mixing ratio from GOMOS and POAM III during the period 1 October 2003-late May 2004 are shown in the lower panel of Figure 1. The upper panel of this figure shows the GOES-measured >10 MeV energy proton fluxes (heavy line), and the K_p index (light line), a measure of geomagnetic activity (Both datasets available through the Space Physics Interactive Data Resource, http://spidr.ngdc.noaa.gov). The middle panel shows the radio wave ionisation index described above, indicating ionisation levels inside the 70-90 km altitude range. GOMOS nighttime NO_2 mixing ratios are shown over 30-70 km altitude from mid-October 2003 through to March 2004. The selected stellar occultations are all located in the polar cap area, in the latitude range 65-85ºN. The GOMOS mixing ratios are determined using neutral densities provided by ECMWF up to 48 km altitude, above which the MSISE-90 model is used. Before November 2003 and after March 2004, there are insufficient nighttime stellar occultations, and therefore POAM III-provided daytime NO_2 measurements over 30-45 km altitude are used, for measurement latitudes >50°N. Note that the strong discontinuity in NO_2 mixing ratios is caused by the difference between nighttime and daytime, due to the diurnal variation of NO_2. Note also that due to the same reason we have applied different colour scales for the GOMOS and POAM III NO_2 datasets. To emphasize the shift from GOMOS nighttime NO_2 to POAM III daytime NO_2, the POAM III measurements are bounded by a heavy line.

The radio wave ionisation index shown in Figure 1 indicates that during the winter there were two principal periods showing significant ionisation increases at ~80 km, which were either created by particle precipitation or by the descent of NO_x from higher altitudes. The first period occurred during the Halloween storm at the end of October 2003, and can be strongly associated with the proton precipitation at that time. The second period occurred at the beginning of January 2004, not associated with any particular storm, but with the strengthening of the polar vortex in the upper stratosphere and consequent strong downward vertical transport. Between mid-December- and early January no significant traces of NO_x can be observed at any altitude.

Although the GOMOS data are sparse during the Halloween storm period it is possible to identify the descent of a region of NO_x enhancement that reaches the upper stratosphere by the beginning of December 2003 (labelled at the initial high altitudes as ‘1’ in Figure 1). The descent of the NO_x enhancement appears to take about 1 month to travel from the mesosphere to 40 km altitude, and the final mixing ratios are about 3× the background levels. This enhancement of NO_x is generated by the Halloween storm proton precipitation, which maximises ionisation rates at altitudes of ~50-80 km, with significant ionization rates down to 30 km and up to 90 km [Jackman et al, 2005]. GOMOS observations of the neutral atmosphere during the Halloween storm period have been presented by Seppälä et al. [2004] and Verronen et al. [2005]. It is known that some solar proton events are also accompanied by a significant population of energetic electrons [Reames, 1995]. However, comparisons between observed NO_x populations and those predicted only from the proton fluxes show good agreement [Jackman et al., 2001, Semeniuk et al., 2005, Clilverd et al., 2006], indicating that the energetic electron population may not be as significant as solar protons deep in the polar cap. In contrast, geomagnetic storms lead to energetic electron precipitation will generally be most significant around the edges of the polar cap where only some protons can reach due to rigidity cutoffs [Rodger et al. 2006], while the protons will affect the majority of the polar cap atmosphere. The Halloween storm is also likely to have produced significant energetic electron precipitation, including relativistic electron precipitation that would penetrate to similar altitudes as the proton precipitation. In terms of significance to the polar atmosphere, the protons are likely to be more important on average. This is consistent with the good agreement between predicted and observed neutral atmosphere variations during the Halloween storm [Verronen et al., 2005], where the modelling only included the GOES-measured proton fluxes. We need to note, however, that our data do not allow the discrimination between the two precipitation mechanisms for this event. The arrival time of the enhancement at 40 km is consistent with the modelling of Semeniuk et al. [2005], and the level of enhancement also agrees with their modelling of NO_x generation through proton precipitation.

Following the initial NO_x enhancement a second period of enhanced NO_x is observed from mid-November to mid-December (labelled ‘2’ in Figure 1). This appears to descend as well, at approximately the same rate as the first NO_x enhancement, but only reaches lower altitudes of 45-50 km before disappearing at all altitudes. During this period there were two small solar proton events (21 Nov and 02 Dec), and several large geomagnetic storms, which could have generated some NO_x at altitudes >60 km, but the timing and altitude range are consistent with the modelling of Semeniuk et al. [2005] when they included enhanced thermospheric ionisation in their calculations (i.e., NO_x generated by low energy electrons) from the Halloween storm and moderately disturbed periods shortly afterward.

A third period of NO_x enhancement starts on 12/13 January 2004 (labelled ‘3’ in Figure 1). First observed at higher altitudes, it can be detected in each instrument in turn until it reaches the upper stratosphere in April 2004. This has previously been described by Randall et al. [2005], Rinsland et al. [2005], and Clilverd et al. [2007]. No single geomagnetic storm or solar proton event can be identified as the cause of the NO_x, and the production altitude appears to be >90 km (auroral energies). The onset date is consistent with the start of strong downward vertical transport in the polar vortex as the upper stratospheric vortex re-strengthens following a stratospheric warming period at the end of December [Clilverd et al., 2006]. The enhancement of NO_x in this third event is 4× the background levels once it reaches 40 km, and is significantly longer-lived than the previous two enhancements, i.e., 4 months compared with 1 month.

During the descent period of the third enhancement a secondary enhancement of NO_x can be seen in mid-February 2004 covering a large range of altitudes (~55-90 km, labelled '4' in Figure 1). The timing of the secondary increase in NO_x is coincident with a large geomagnetic storm that occurred on 11 Feb, which had no associated solar proton event. The NO_x enhancements are significant, and add to the already descending NO_x at 50-55 km, but disappear at higher altitudes after about one week. This secondary enhancement is clearly the result of energetic electron precipitation generating NO_x at altitudes of ~55-70 km, i.e., electron energies of 200-1000 keV.

In order to determine the significance of the NO_x enhancements to stratospheric ozone loss, we examine the time variation of stratospheric and mesospheric O_3 during the same time period. Figure 2 shows measurements of the northern hemisphere polar O_3 mixing ratios over the altitude range 30-60 km. Nighttime O_3 measurements from GOMOS are shown for the period November 2003 to March 2004, with daytime O_3 measurements from POAM III also included as indicated in the figure. Figure 3 shows the polar O_3 mixing ratios at various selected altitudes. The upper panel shows the latitudes of the occultation measurements for the two different instruments. The average long term O_3 mixing ratio at 40 km is presented from the 9-year POAM average from 1994-2003 (green line) taken from Figure 1 of Randall et al. [2005]. Also shown, as a reference showing the seasonal variability, is the O_3 mixing ratio at 30 and 40 km and 70°N (shown in the upper panel by a red line) from the FinROSE CTM (red line) [Damski et al., 2007a, 2007b], which includes no particle forcing. FinROSE is a global 3D (in this study we have used results from model run with 5°×10° grid and 32 vertical pressure levels from surface to 0.1 hPa) grid point, off-line chemistry transport model driven by ECMWF model winds and includes 114 gas-phase reactions, 37 photodissociation processes and 10 heterogeneous reactions for 28 long-lived species/families and 15 species in photochemical equilibrium. To compensate for the known O_3 deficit in the model results, we have increased the values by 10%, leading to reasonable agreement with the 9-year POAM average when POAM is observing similar latitudes. These mixing ratios are to be contrasted with measurements taken during October 2003 to June 2004 by the GOMOS (black line, nighttime) and POAM III (blue line, daytime) instruments. The standard deviations of these measurements are shown by the dotted envelopes. In both Figure 2 and 3 there is good agreement between GOMOS and POAM III during the October-November and February-March transitions in the stratosphere when the observation latitudes are similar, but poor agreement around and above the stratopause (50 km), due to the diurnal variation of O_3 in the mesosphere. Thus we can contrast the levels of stratospheric O_3 measured by the two different instruments across the time period shown in these figures.

The winter 2003/2004 ozone levels shown at 40 km in Figure 3 indicate that a significant decrease occurs from mid-November until almost the end of December, particularly at higher latitudes. The average ozone mixing ratios are reduced from 5 to 3.5 ppmv as a result of the NO_x descent following the Halloween storm (event '1') and also a contribution from the continuing descent of NO_x through November seen in event '2'. The recovery of the ozone and the loss of NO_x towards the end of December 2003 are likely to be caused by the start of the sudden stratospheric warming period, with a consequent mixing of O_x rich mid-latitude air into the polar vortex.

The POAM measurements in Figure 3 also show decreases from average levels in April and May 2004, as earlier shown by Randall et al. [2005]. Note that it is less valid to contrast the FinROSE model results for this time period, due to the latitudinal difference. The observed mixing ratios reduce from 6 to 5 ppmv by the end of April. This is a result of the descent of NO_x that started in the auroral altitudes in early January 2004 (event '3'), with a contribution from the geomagnetic storm of 11 February 2004 (event '4'). There is also evidence of the impact of NO_x

on the ozone levels at 50 km altitude during the descent period. Decreases in ozone mixing ratios can be seen at 50 km at the beginning of March 2004.

At 30 km altitudes no significant changes in ozone mixing ratio can be seen in November/December through to April/May. There is some difference between GOMOS and POAM III in December, suggesting some impact of the Halloween storm at 30 km at higher latitudes (75º-85º) but not equatorward of that. This is consistent with the containment of most of the NO_x descent to ~40 km altitudes (Figure 1), particularly in the case of the January-May descent period.

We have shown that there are two main features in the upper stratosphere ozone levels during the winter 2003/04, particularly at 40 km altitudes. Two periods show low levels of ozone, namely December 2003 and April 2004. The first minima is deep in the winter period following the Halloween storm, both as a result of proton and electron precipitation to low altitudes (~50 km) and subsequent enhanced auroral activity through November 2003. A recovery of ozone is seen during January-March 2004, which is consistent with the normal behaviour of ozone determined from past data. In April 2004 ozone levels decrease significantly compared with the normal levels for the time of year. This is the result of the descent of LEE-NO_x that started in January 2004, and possibly the additional effect of high-energy electron precipitation that supplemented the NO_x levels on 11 February 2004.

4. Discussion

During the northern hemisphere polar winter of 2003 to 2004 four significant enhancements of NO_x in the upper stratosphere were observed following either solar proton precipitation events, energetic electron precipitation events, or the descent of LEE-NO_x. In turn these NO_x enhancements caused two reductions in ozone in the upper stratosphere. NO_x events '1' and '2' combined to produce ozone loss at 40 km altitude during November and December 2003, while NO_x events '3' and '4' combined to produce the reduction in ozone observed in April and May 2004. The ozone loss at 40 km was 1-1.5 ppmv (up to 30%), relative to the average ozone levels expected for that time of year, and lasting for about 1 or 2 months. If compared to pre-solar proton event O_3 levels, there is a 60% decrease in November-December 2003 consistent with GOMOS observations reported by Seppälä et al. [2004], some of this being due to seasonal variation as seen from the FinROSE model results.

In terms of the impact at stratospheric altitudes it is difficult to single out the most significant event. The combination of NO_x events '1' and '2' in November 2003 was dominated by event '1' in terms of reaching 40 km altitude, as event '2' was still descending towards these altitudes when the upper stratospheric warming started. The combination of NO_x events '3' and '4' in April 2004 are less easy to separate. Event '4' clearly added to the NO_x already present as a result of event '3', and both were able to descend to 40 km altitude.

The two NO_x enhancement events ('2' and '4' in Figure 1) were most likely generated by energetic electron precipitation associated with geomagnetic storms, although some contribution from descending LEE-NO_x in November 2003 appears to be consistent with model results [Semeniuk et al., 2005]. In both these cases the stratospheric impact of the NO_x is uncertain as no clear signature was observed at altitude <45 km, partly as a result of a reduction of strong vertical downward transport during a stratospheric warming event at the end of December 2003 (event '2'), and partly because of the effect of photolysis of the NO_x at high altitudes during the lengthening daylight hours in late February (event '4').

Sources of ionisation that could generate NO_x enhancements have significant differences in geographical location. Solar proton events typically generate ionisation uniformly over the pole at geographic latitudes >60°N as they access the atmosphere directly from the Sun but are guided by the Earth's magnetic field to the polar regions [Störmer, 1930, Rodger et al., 2006]. Electron precipitation can affect the regions between the L-shells 3<L<8 (invariant latitudes of about 55-70°), both in terms of LEE-NO_x generation and upper stratosphere/mesosphere generation. In geographical coordinates in the northern hemisphere this relates to ~45-75°N. This latitudinal restriction comes from the amplification of solar wind conditions by magnetospheric processes that lead to energetic particle precipitation into the atmosphere [Callis et al., 1998]. Our NO_x measurements are typically located between latitudes of 60-75°N, which makes them well placed for NO_x generated by low energy electron precipitation and energetic electron precipitation, leaving out the higher latitudes of the polar cap where NO_x would principally be generated by energetic solar proton precipitation.

At very high latitudes any NO_x generated by, for example, the Halloween storm could survive for many months, as losses due to photolysis are negligible in the dark winter pole. It is possible therefore that the descent of the NO_x enhancement in January 2004 (event '3') could be due to the horizontal transport of NO_x at mesospheric altitudes from the dark pole to the observation latitudes (60-75°N) and then transported downwards to the upper stratosphere [Natarajan et al., 2004].

In Figure 4 we show GOMOS data from a range of latitude bands zonally averaged during the winter of 2003-04. The top latitude band is from 75-85°N, the middle latitude band is 65-75°N, and the lowest latitude band is 55-65°N. The plot shows that at very high latitudes (65-75°N and 75-85°N) no hidden reservoir of NO_x below 70 km can be detected in the period prior to 12/13 January when descending NO_x is observed. This is consistent with a picture of descending LEE-NO_x generated by electron precipitation from continuing geomagnetic activity during the late-December/early-January period rather than NO_x preserved at the dark winter pole after its generation by the Halloween storm in late-October. Limited data coverage at these high latitudes prevents us from making any conclusions about the latitude range of the energetic electron precipitation observed in the middle panel in mid-Feb (event '4').

5. Summary

In this paper we report GOMOS, POAM III, and radio wave observations of polar middle atmosphere NO_x during the northern hemisphere winter of 2003-04. Four significant enhancements of NO_x in the upper stratosphere were observed following either solar proton precipitation events, or energetic electron precipitation events, or the descent of LEE-NO_x. All of these production processes are likely to be associated with geomagnetic disturbances (e.g., A_p).

The most significant events at upper stratospheric altitudes (~40 km) were the descent of LEE-NO_x in January 2004 initiated by downward vertical transport resulting from the strengthening of the polar vortex, and the very large solar proton event associated with the Halloween storm in October 2003. A sudden stratospheric warming in late December 2003 may have disrupted the cumulative stratospheric effect of the Halloween storm. The importance of the NH polar vortex in transporting the high altitude NO_x to lower altitudes has recently been recognized as exceptionally high NO_x amounts have been observed in the NH polar stratosphere following exceptional meteorological conditions affecting the polar vortex (NH early 2004 and 2006) [Randall et al., 2006]. GOMOS observations made at very high latitudes showed that no reservoir of NO_x generated by proton precipitation was detectable at the dark winter pole to provide a source of NO_x for the January 2004 NO_x descent.

The other two NO_x enhancement events were most likely generated by energetic electron precipitation associated with geomagnetic storms. The stratospheric impact of the NO_x generated in this way is uncertain as no clear enhancement of NO_x was observed at altitudes <50 km. However, the events were either limited by the mid-winter stratospheric warming event, or overlaid by the January 2004 NO_x descent event, or by occurring late in the winter period and being dissipated by photolysis effects on the NO_x at altitudes >60 km.

The four NO_x enhancements combined to cause two reductions in ozone in the upper stratosphere. NO_x events '1' and '2' produced ozone loss at 40 km altitude during November and December 2003, while NO_x events '3' and '4' produced reduced ozone in April and May 2004. The ozone loss at 40 km was 1-1.5 ppmv (up to 30%), relative to the average ozone levels expected for that time of year, and lasting for about 1 or 2 months. Clearly the interplay between the production of thermospheric and mesospheric NO_x with ozone losses in the upper stratosphere is complex and depends on the timing of each relative to the others, combined with the effects of sudden stratospheric warmings. The role of the polar vortex in transporting the NO_x downwards is critical and ultimately limits the influence of all NO_x source processes in the stratosphere.

Appendix A - GOMOS data selection

This appendix discusses the GOMOS data selection criteria and the GOMOS data accuracy.

As was noted in section 2, for this study we selected GOMOS measurements using the following criteria 1) nighttime measurements, i.e. the solar zenith angle at the tangent point is >107° and the solar zenith angle at the satellite point is >90° (to avoid stray light), 2) measurement location in the Northern Hemisphere polar area at latitudes ≥ 65°N and at latitudes 55°N-65°N, and 3) the temperature of the star used in the occultation is > 6000 K for both NO_2 and O_3 measurement to provide identical spatial and temporal distribution of the measurements of the different gases for comparison. With these restrictions over 2000 individual occultations were selected. Figure A1 presents the temperatures and magnitudes of the stars used in the occultations with respect to time and the measurement latitude. In the bottom panel of Figure A1 is shown the number of used occultations per star. More than 1000 occultations were made using the brightest available star, Sirius (Star ID 1, magnitude -1.44). The Star ID numbers in Figure A1 correspond to the (visual) magnitude of the star so that number 1 corresponds to the brightest star. Figures A2 and A3 show the relative accuracies of the averaged GOMOS NO_2 and O_3 measurements shown in Figures 1, 2 and 4. The relative accuracies of the averaged measurements were calculated according to

$$\sigma_{\bar{x}}^2 = \frac{1}{N^2}\sum_{i=1}^{N}\sigma_{x_i}^2 \qquad \text{(A1.1)}$$

where $\sigma_{x_i}^2$ are the variances of the individual measurements $x_i, i = 1,\ldots,N$. The lower parts of the panels in Figure A2 show the number of occultations used in each point in the average. In the three latitude bands shown in the figure (55-65°N, 65-75°N and 75-85°N) approximately 30 occultations per point are used. As seen from Figures 4 and A2 the accuracy is good for the observed NO_2 enhancements in Nov-Dec 2003 and Jan-Feb 2004, for example for the descending NO_2 in Jan 2004 the accuracy is better than 20% (for 80 ppbv this corresponds to accuracy of 16 ppbv) and in Feb 2004, when the enhancement reaches the stratosphere the accuracy is 2-5%. For the lower latitudes 55-65°N where the NO_2 signal is weaker at high altitudes than it is at the higher latitudes, the accuracy is >40% above 50 km. This is expected as in typical polar conditions when high amounts of NO_x do not exist in the upper stratosphere-lower mesosphere, the GOMOS NO_2 profiles are considered to extend from 20 to 50 km, as above 50km the NO_2 signal weakens rapidly. In contrast, during times when strong NO_x enhancements occur the altitude range of the NO_2 measurements extends up to 70 km [Hauchecorne et al., 2005]. Figure A3 shows the relative accuracy of the GOMOS O_3 results shown in Figure 2. Above 45 km the accuracy is better than 0.5% while between 40 and 45 km the accuracy is between 1.5-0.5%.

Acknowledgments. The work of A.S. was supported by the Academy of Finland (Middle Atmosphere Interactions with Sun and Troposphere). We are grateful to Laura Thölix for providing the FinROSE results. We would also like to thank all researchers involved in the development and validation of the POAM III instrument as well as the GOMOS team. A.S. thanks the GOMOS Quality Working Group members E. Kyrölä, V. F. Sofieva and J. Tamminen for helpful discussions concerning GOMOS measurements.

References

Callis, L. B., M. Natarajan, D. S. Evans, J. D. Lambeth (1998), Solar atmospheric coupling by electrons (SOLACE) 1. Effects of the May 12, 1997 solar event on the middle atmosphere, *J. Geophys. Res*., 103(D21), 28405-28420, doi: 10.1029/98JD02408.

Clilverd, M. A., C. J. Rodger, T. Ulich, A. Seppälä, E. Turunen, A. Botman, and N. R. Thomson (2005), Modeling a large solar proton event in the southern polar atmosphere, *J. Geophys. Res*., 110, A09307, doi: 10.1029/2004JA010922.

Clilverd, M.A., Seppälä, A., Rodger, C. J., Thomson, N.R., Verronen, P., Turunen, E., Ulich, Th., Lichtenberger, J., and Stienbach, P. (2006), Modeling polar ionospheric effects during the October-November 2003 solar proton events, *Radio Sci*., 41, RS2001, doi: 10.1029/2005RS003290.

Clilverd, M. A., A. Seppälä, C. J. Rodger, P. T. Verronen, and N. R. Thomson (2006), Ionospheric evidence of thermosphere-to-stratosphere descent of polar NO_x, *Geophys. Res. Lett*., 33, L19811, doi:10.1029/2006GL026727.

Clilverd, M. A., A. Seppälä, C. J. Rodger, N. R. Thomson, and J. Lichtenberger (2007), Temporal variability of the descent of high-altitude NO_x inferred from ionospheric data, In press, *J. Geophys. Res.*

Damski, J., L. Thölix, L. Backman, P. Taalas, and M. Kulmala (2007a), FinROSE – Middle atmospheric chemistry transport model. In press, *Boreal Environment Research*.

Damski J., L. Thölix, L. Backman, J. Kaurola, P. Taalas, J. Austin, N. Butchart, M. Kulmala (2007b), A chemistry-transport model simulation of middle atmospheric ozone from 1980 to 2019 using coupled chemistry GCM winds and temperatures, *Atmos. Chem. Phys. Discuss*., 7, 1143-1181.

Funke, B., M. Lopez-Puertas, S. Gil-Lopez, T. von Clarmann, G. P. Stiller, H. Fischer, and Kellmann (2005), Downward transport of upper atmospheric NO_x into the polar stratosphere and lower mesosphere during the Antarctic 2003 and Arctic 2002/2003 winters, *J. Geophys. Res*., 110 (D24), D24308, doi: 10.1029/2005JD006463.

Hauchecorne, A., et al. (2005), First simultaneous global measurements of nighttime stratospheric NO2 and NO3 observed by Global Ozone Monitoring by Occultation of Stars (GOMOS)/Envisat in 2003, *J. Geophys. Res*., 110, doi: 10.1029/2004JD005711.

Hauchecorne, A., J-L. Bertaux, F. Dalaudier, J. M. Russell III, M. G. Mlynczak, E. Kyrölä, and D. Fussen (2007), Large increase of NO_2 in the north polar mesosphere in January-February 2004: Evidence of a dynamical origin from GOMOS/ENVISAT and SABER/TIMED data, *Geophys. Res. Lett.*, 34, L03810, doi:10.1029/2006GL027628.

Hedin, A. E (1991), Extension of the MSIS Thermospheric Model into the Middle and Lower Atmosphere, *J. Geophys. Res*., 96, 1159-117.

Jackman, C. H., M. T. DeLand, G. J. Labow, E. L. Fleming, D. K. Weisenstein, M. K. W. Ko, M. Sinnhuber, and J. M. Russell (2005), Neutral atmospheric influences of the solar proton events in October-November 2003, *J. Geophys. Res*., 110, A09S27, doi: 10.1029/2004JA010888.

Jackman, C. H., R. M. McPeters, G. J. Labow, E. L. Fleming, C. J. Praderas, and J. M. Russell (2001), Northern hemisphere atmospheric effects due to the July 2000 solar proton event, *Geophys. Res. Lett*., 28, 2883-2886.

Kyrölä, E., et al. (2004), GOMOS on Envisat: An overview, *Adv. Space Res*., 33, 1020-1028.

Kyrölä, E., et al. (2006), Nighttime ozone profiles in the stratosphere and mesosphere by Global Ozone Monitoring by Occultation of Stars on Envisat, *J. Geophys. Res*., 111, D24306, doi: 10.1029/2006JD007193.

Lopez-Puertas, M., B. Funke, S. Gil-Lopez, T. v. Clarmann, G. P. Stiller, M. Höpfner, S. Kellmann, H. Fischer, and C. H. Jackman (2005), Observation of NO_x enhancement and ozone depletion in the northern and southern hemispheres after the October-November 2003 solar proton events, *J. Geophys. Res*., 110, A09S43, doi: 10.1029/2005JA011050.

Manney, G. L., K. Kruger, J. L. Sabutis, S. A. Sena, and S. Pawson (2005), The remarkable 2003-2004 winter and other recent warm winters in the Arctic stratosphere since the late 1990s, *J. Geophys. Res*., 110, D04107, doi: 10.1029/2004JD005367.

Natarajan, M., E. E. Remsberg, L. E. Deaver, and J. M. Russell (2004), Anomalously high levels of NO_x in the polar upper stratosphere during April, 2004: Photochemical consistency of HALOE observations, *Geophys. Res. Lett*., 31, L15113, doi: 10.1029/2004GL020566.

Randall, C. E., et al. (2002), Validation of POAM III NO2 measurements, *J. Geophys. Res.*, 107(D20), 4432, doi: 10.1029/2001JD001520.

Randall, C. E., et al. (2003), Validation of POAM III ozone: Comparisons with ozonesonde and satellite data, *J. Geophys. Res*., 108(D12), 4367, doi: 10.1029/2002JD002944.

Randall, C. E., et al. (2005), Stratospheric effects of energetic particle precipitation in 2003-2004, *Geophys. Res. Lett*., 32, L05802, doi:10.1029/2004GL022003.

Randall, C. E. V. L. Harvey, C. S. Singleton, P. F. Bernath, C. D. Boone, and J. U. Kozyra (2006), Enhanced NO_x in 2006 linked to strong upper stratospheric Arctic vortex, *Geophys. Res. Lett*., 33, L18811, doi: 10.1029/2006GL027160.

Reames, D. V. (1995), Solar Energetic Particles: A Paradigm Shift, *Rev. Geophys. (Suppl.),* 33, 585.

Renard, J-B., P-L. Blelly, Q. Bourgeois, M. Chartier, F. Goutail, and Y. J. Orsolini (2006), Origin of the January–April 2004 increase in stratospheric NO_2 observed in the northern polar latitudes, *Geophys. Res. Lett*., 33, L11801, doi:10.1029/2005GL025450.

Rodger, C. J., M. A. Clilverd, P. T. Verronen, Th. Ulich, M. J. Jarvis, and E. Turunen (2006), Dynamic geomagnetic rigidity cutoff variations during a solar proton event, *J. Geophys. Res.*, 111, A04222, doi: 10.1029/2005JA011395.

Semeniuk K., J. C. McConnell, C. H. Jackman (2005), Simulation of the October–November 2003 solar proton events in the CMAM GCM: Comparison with observations, *Geophys. Res. Lett*., 32, L15S02, doi:10.1029/2005GL022392.

Seppälä, A., P. T. Verronen, E. Kyrölä, S. Hassinen, L. Backman, A. Hauchecorne, J. L. Bertaux, and D. Fussen (2004), Solar Proton Events of October-November 2003: Ozone depletion in the Northern hemisphere polar winter as seen by GOMOS/Envisat, *Geophys. Res. Lett.*, 31 (19), L19107, doi:10.1029/2004GL021042.

Seppälä, A., P. T. Verronen, V. F. Sofieva, J. Tamminen, E. Kyrölä, C. J. Rodger, and M. A. Clilverd (2006), Destruction of the tertiary ozone maximum during a solar proton event, *Geophys. Res. Lett.*, 33, L07804, doi: 10.1029/2005GL025571.

Solomon S, G. C. Reid, R. G. Roble, and P. J. Crutzen (1982), Photochemical coupling between the thermosphere and the lower atmosphere. I - Odd nitrogen from 50 to 120 km, *J. Geophys. Res.*, 87, 7206-7220.

Störmer, C. (1930), Periodische Elektronenbahnen im Feld eines Elementarmagnetron und ihre Anwendung auf Bruches Modellversuche und auf Eschenhagens Elementarwellen des Erdmagnetismus, *Zeitschr. f. Astrophys.*, 1, 237-274.

Verronen , P. T., A. Seppälä, M. A. Clilverd, C. J. Rodger, E. Kyrölä, C. F. Enell, Th. Ulich, and E. Turunen (2005), Diurnal variation of ozone depletion during the October-November 2003 solar proton event, *J. Geophys. Res.*, 110(A9), doi: 10.1029/2004JA010932.

M. A. Clilverd, Physical Sciences Division, British Antarctic Survey, High Cross, Madingley Road, Cambridge CB3 0ET, England, U.K. (e-mail: macl@bas.ac.uk)

C. J. Rodger, Department of Physics, University of Otago, P.O. Box 56, Dunedin, New Zealand. (email: crodger@physics.otago.ac.nz)

A. Seppälä, Earth Observation, Finnish Meteorological Institute, P.O. Box 503, FI-00101 Helsinki, Finland (email: annika.seppala@fmi.fi)

Figures

Figure 1. Combined observations of NO_2 during the northern hemisphere winter 2003-2004. The upper panel shows the >10 MeV proton flux (heavy line) and K_p index (light line). The middle panel indicates high altitude ionisation levels determined from the subionospheric radio wave index. The lower panel shows GOMOS nighttime and POAM III daytime NO_2 mixing ratios, with the POAM data shown inside heavy boxes. Both datasets have been zonally averaged over two days. Note the differing colour scales for the two satellite datasets. These observations show the generation and descent of NO_x into the upper stratosphere.

Figure 2. Combined observations of O_3 from GOMOS and POAM III. Both datasets have been zonally averaged over two days.

Figure 3. Measurements of the northern hemisphere polar O_3 mixing ratios at altitudes between 30-50 km. The upper panel shows the latitudes of the occultation measurements and the model location. The average long term O_3 mixing ratio is presented at the 40 km level from the POAM average (green line) and together with that from the FinROSE model (red line), also shown at the 30 km level. These are to be contrasted with the O_3 mixing ratios measured during October 2003 to June 2004 by the GOMOS (black line, nighttime) and POAM III (blue line, daytime) instruments.

Figure 4. GOMOS NO_2 zonally, and over two days averaged mixing ratio [ppbv] data for the northern hemisphere winter 2003-2004 for three latitude bands (top to bottom) 75-85°N, 65-75°N, 55-65°N.

Figure A1. Selected GOMOS measurements. Top: Temperatures [K] of the stars used in the selected occultations with respect to time and latitude of the occultation. Middle: Visual magnitudes of the stars used in the selected occultations with respect to time and latitude of the occultation. Bottom: Number of occultations per star presented using the GOMOS Star ID numbers from 1 to 130. The star numbering is based on the visual magnitude if the star, starting from the brightest star (Star 1, visual magnitude -1.44).

Figure A2. The relative accuracy [%] of the GOMOS NO_2 measurements presented in Figure 4. The contour lines are plotted for 2, 5, 20, and 40%. The lower parts of each panel present the number of occultations used in the averaging. The GOMOS NO_2 measurements presented in Figure 1 correspond to the two upper-most panels.

Figure A3. The relative accuracy [%] of the GOMOS O_3 measurements presented in Figure 2. The contour lines are plotted for 0.5, 1, 1.5, 2, 2.5, and 3%.

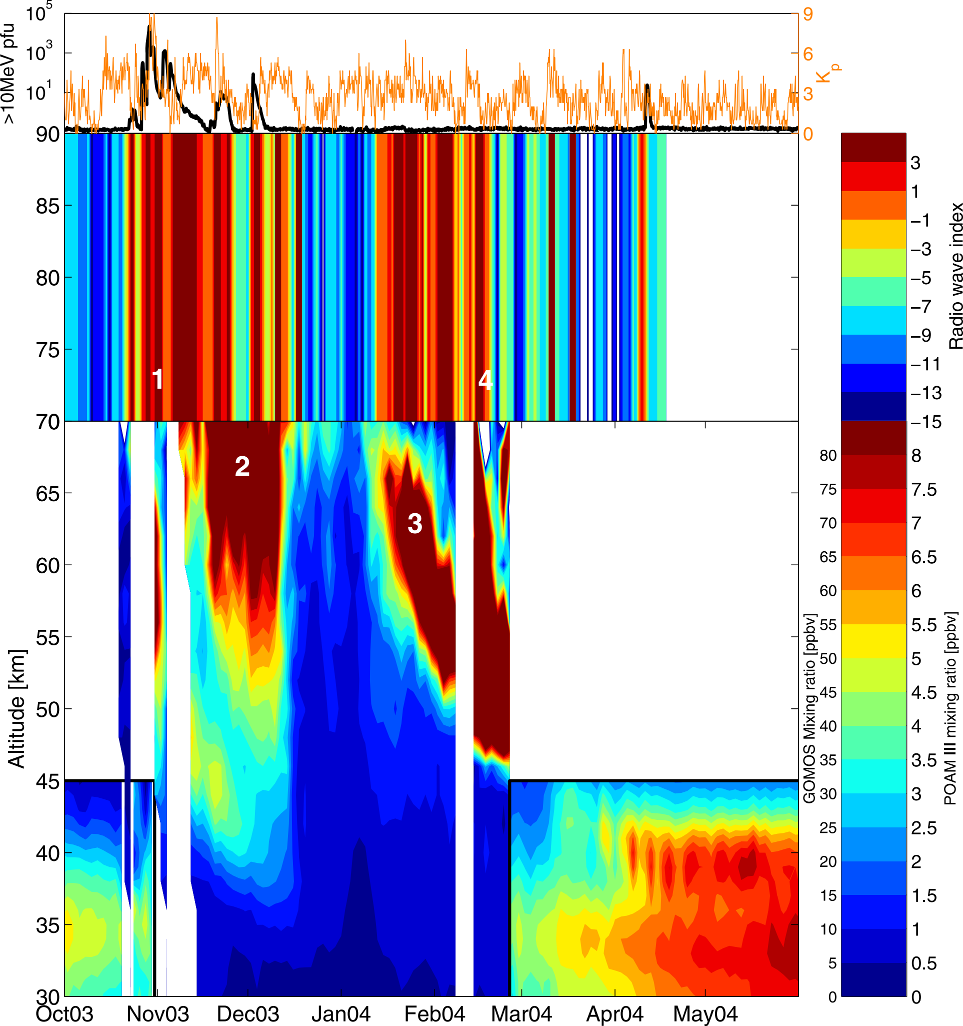

>10MeV pfu
Kp
Radio wave index
Altitude [km]
GOMOS Mixing ratio [ppbv]
POAM III mixing ratio [ppbv]
1
2
3
4
Oct03
Nov03
Dec03
Jan04
Feb04
Mar04
Apr04
May04

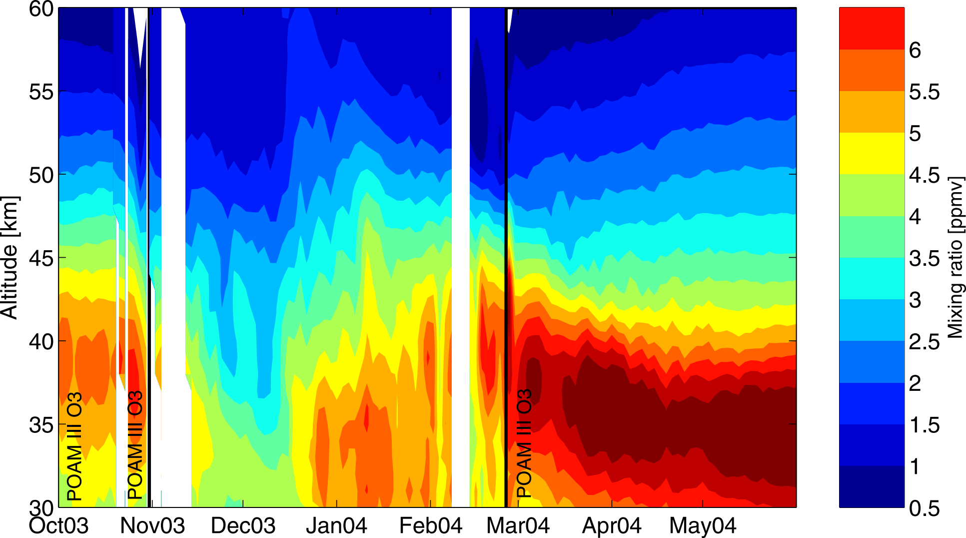

60
55
50
45
40
35
30
Altitude [km]
Oct03
Nov03
Dec03
Jan04
Feb04
Mar04
Apr04
May04
POAM III O3
POAM III O3
POAM III O3
6
5.5
5
4.5
4
3.5
3
2.5
2
1.5
1
0.5
Mixing ratio [ppmv]

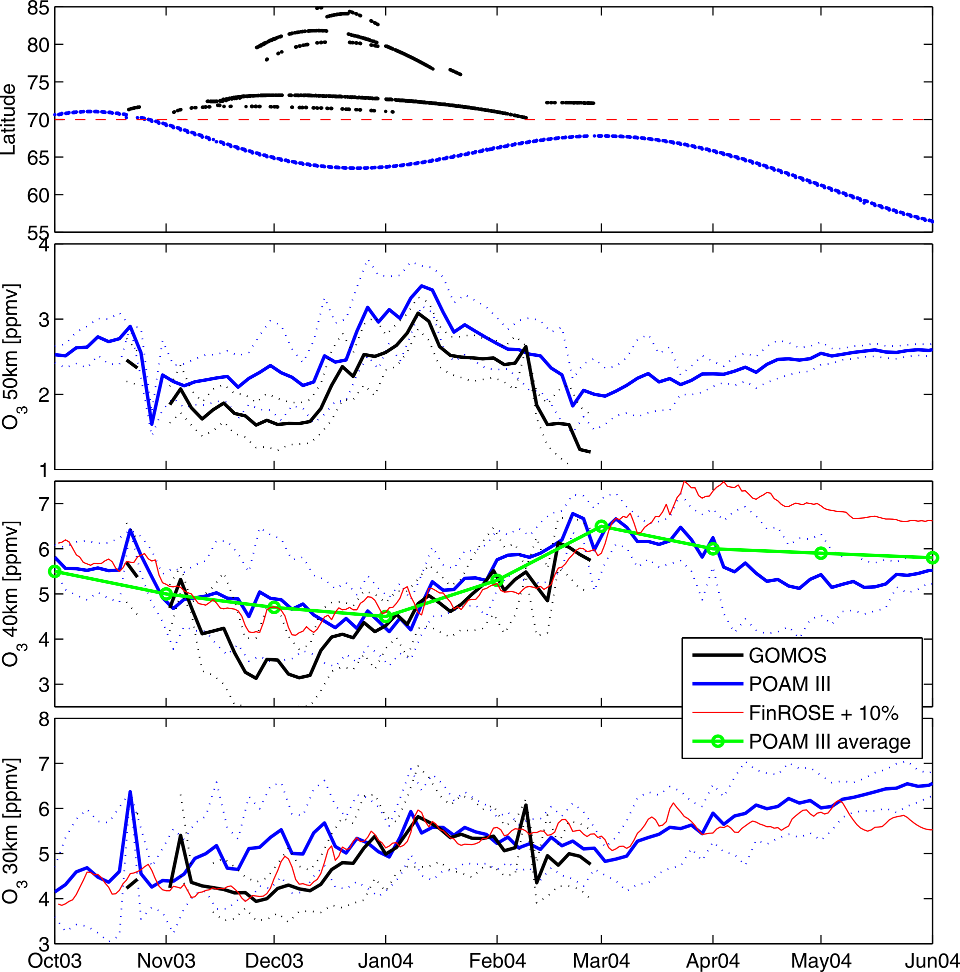

Latitude
O3 50km [ppmv]
O3 40km [ppmv]
O3 30km [ppmv]
GOMOS
POAM III
FinROSE + 10%
POAM III average
Oct03
Nov03
Dec03
Jan04
Feb04
Mar04
Apr04
May04
Jun04

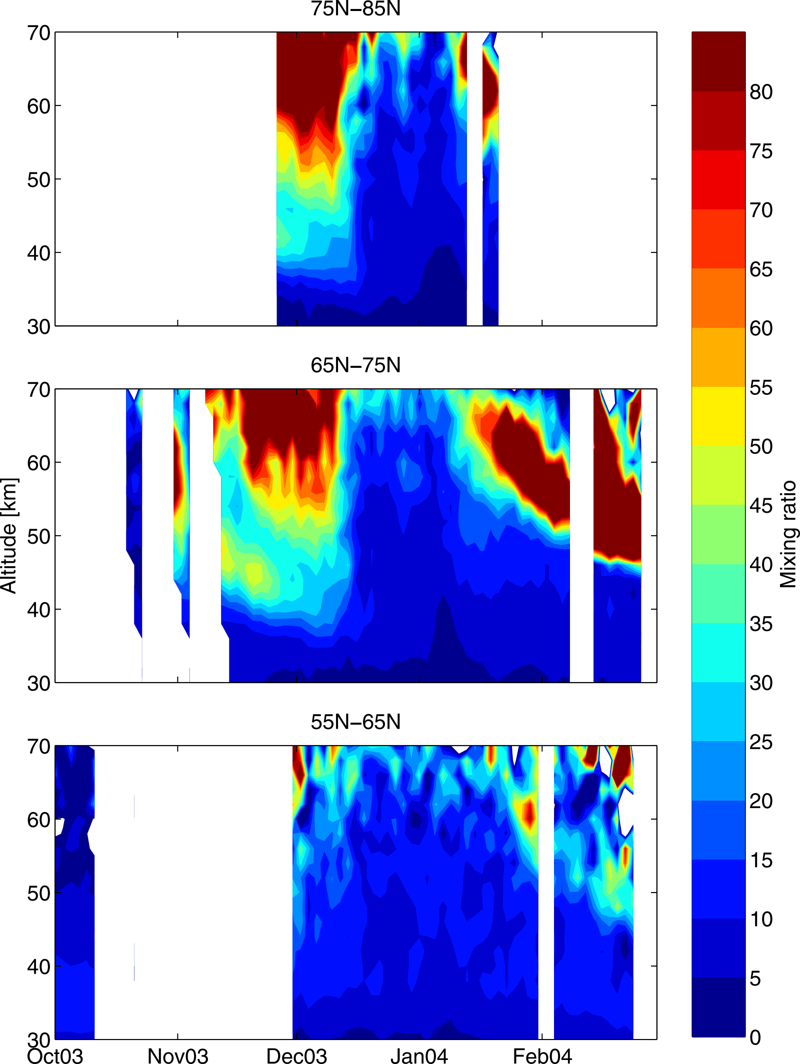
75N–85N
65N–75N
55N–65N
Altitude [km]
70
60
50
40
30
Oct03
Nov03
Dec03
Jan04
Feb04
Mixing ratio
0
5
10
15
20
25
30
35
40
45
50
55
60
65
70
75
80